

Feedback-Topology Designs for Interference Alignment in MIMO Interference Channels

Sungyoon Cho, Hyukjin Chae, Kaibin Huang, Dongku Kim, Vincent K. N. Lau, Hanbyul Seo
and Byounghoon Kim

Abstract

Interference alignment (IA) is a joint-transmission technique that achieves the capacity of the interference channel for high signal-to-noise ratios (SNRs). Most prior work on IA is based on the impractical assumption that perfect and global channel-state information(CSI) is available at all transmitters. To implement IA, each receiver has to feed back CSI to all interferers, resulting in overwhelming feedback overhead. In particular, the sum feedback rate of each receiver scales quadratically with the number of users even if the quantized CSI is fed back. To substantially suppress feedback overhead, this paper focuses on designing efficient arrangements of feedback links, called *feedback topologies*, under the IA constraint. For the multiple-input-multiple-output (MIMO) K -user interference channel, we propose the feedback topology that supports sequential CSI exchange (feedback and feedforward) between transmitters and receivers so as to achieve IA progressively. This feedback topology is shown to reduce the network feedback overhead from a cubic function of K to a linear one. To reduce the delay in the sequential CSI exchange, an alternative feedback topology is designed for supporting two-hop feedback via a control station, which also achieves the linear feedback scaling with K . Next, given the proposed feedback topologies, the feedback-bit allocation algorithm is designed for allocating feedback bits by each receiver to different feedback links so as to regulate the residual interference caused by the finite-rate feedback. Simulation results demonstrate that the proposed bit allocation leads to significant throughput gains especially in strong interference environments.

Index Terms

Interference alignment, degrees of freedom, MIMO, interference channels, feedback topology, limited feedback, bit allocation

S. Cho, H. Chae, K. Huang and D. Kim are with the school of EEE, Yonsei University, Korea; V. K. N. Lau is with the dept. of ECE, Hong Kong University of Science and Technology, Hong Kong; H. Seo and B. Kim are with the Advanced Communication Technology Lab, LG Electronics, Korea. Corresponding author: K. Huang (email: huangkb@yonsei.ac.kr, huangkb@me.com).

I. INTRODUCTION

In a wireless interference network, interference alignment (IA) maximizes the number of decoupled data links, called *degrees of freedom* (DoF), by aligning the cross-link interference signals for each user in a subspace of the signal space extended over time, frequency or space. Such alignment requires the acquisition of perfect and global channel state information at transmitters (CSIT), incurring potentially overwhelming CSI feedback overhead in practice. Therefore, the efficient CSIT acquisition remains the key challenge for implementing IA techniques and is the main theme of this paper. Specifically, efficient arrangements of CSI feedback links, called *feedback topologies*, are proposed for reducing the sum feedback overhead for IA. This overhead is further reduced by dynamically distributing CSI bits over feedback links under a sum feedback constraint.

The original IA techniques achieve the maximum DoF of the K -user single-antenna interference channel, namely $K/2$, by asymptotic signal-space expansion to attain the ergodicity of the channel variation in time or frequency, called *symbol extension* [1]–[3]. Given symbol extension, the bounds on the achievable DoF for multiple-input-multiple-output (MIMO) interference channel were derived in [4], [5] and the optimal IA solutions were obtained in closed-form for some specific settings. Due to the impracticality of symbol-extension, recent IA research has been focusing on quantifying the achievable DoF and designing matching IA solutions for a single realization of the MIMO interference channel, called the *MIMO constant channel* [6]–[10]. In particular, the IA feasibility conditions were derived in [6]–[8] and iterative IA algorithms for achieving such conditions were proposed in [9], [10], which exploit the channel reciprocity to achieve distributive implementation. In addition, the IA principle has been extended to design multi-cell precoding for cellular networks [11]–[14].

In practice, CSIT required for IA usually has to rely on finite-rate CSI feedback, called *limited feedback*, from receivers to their interferers, resulting in imperfect CSIT. The required scaling laws of the number of feedback bits per user for the IA algorithms to achieve the maximum DoF have been derived in [15], [16]. In the literature of limited feedback, comprehensive limited feedback algorithms have been designed for the single-user (see e.g., [17]–[21]) and multi-user MIMO systems (see e.g., [22]–[24]). However, there are few practical algorithms for limited feedback targeting IA, which motivates the current work.

This paper considers the K -user constant MIMO interference channel where each transmitter/receiver employs M antennas. Based on the closed-form solution of IA precoders, we propose the feedback topologies which can be implemented by a finite-rate CSI feedforward and feedback links. The contributions of this paper are summarized as follows.

- 1) We propose *CSI-exchange feedback topology* where the IA precoders are sequentially computed based on the exchange of pre-determined precoders (under the existence of feedforward/feedback

channels) between subsets of transmitters and receivers. In the proposed feedback design, the total number of complex coefficients for CSI exchange, referred to as *CSI overhead*, is shown to scale with the number of users K *linearly* rather than *cubically* for the conventional approach where each receiver feeds back the CSI to all transmitters through the feedback links for the computation of IA precoder [1]-[5]. As a result, the proposed CSI-exchange feedback topology yields dramatic reduction of CSI overhead especially when K is large.

- 2) While the proposed CSI-exchange feedback method is efficient for the reduction in the CSI overhead, the sequential operation may incur significant delay, which is highly undesirable. To address this issue, we further propose the *star feedback topology* where a CSI control station collects CSI from all receivers, computes the IA precoders, and then communicate them to the transmitters. Compared with the CSI-exchange feedback topology, the current design requires only two step CSI feedback without CSI feedforward and hence, it can reduce the associated delay.
- 3) For practical implementations, we consider the impact of limited feedback on the performance of the feedback topology in the interference network. Assuming that random vector quantization (RVQ) in [21] is used for quantizing CSI, the expected cross-link interference power at each receiver is upper-bounded by sum of exponential functions of the numbers of feedback bits sent by the receiver. Both the CSI-exchange and star feedback topologies are considered in the analysis.
- 4) Minimizing the upper bounds on the above interference power gives a dynamic feedback-bit allocation algorithm based on the water-filling principle. Such an algorithm is shown to provide significant capacity gains over the uniform feedback-bit allocation especially for high SNR's.
- 5) Using the proposed feedback topology schemes, we derive the required number of feedback bits sent by each receiver for achieving the same DoF as the case of perfect CSIT, which increases linearly with K and logarithmically with the transmission power.

The remainder of this paper is organized as follows. In Section II, the system model is described. The three CSI feedback topologies are proposed in Section III. The effect of CSI-feedback quantization is analyzed and the dynamic feedback-bit allocation algorithm is proposed in Section IV and V, respectively. Section VI provides simulation results and the concluding remarks are followed in Section VII.

II. SYSTEM MODEL

We consider K pairs MIMO interference channel where each node has M antennas and delivers d data streams to the target receiver over a common spectrum. The wireless channels are characterized by path-loss and small-scale fading and all channel-fading coefficients are assumed to be independent and identically distributed (i.i.d) circularly symmetric complex Gaussian random variables with zero mean

and unit variance, denoted as $\mathcal{CN}(0, 1)$. Let the $M \times M$ matrix $\mathbf{H}^{[kj]}$ group the fading coefficients of the channel from transmitter j to receiver k and thus $\mathbf{H}^{[kj]}$ comprises i.i.d. $\mathcal{CN}(0, 1)$ elements. Then, the channel from transmitter j to receiver k can be readily written as $d_{kj}^{-\alpha/2} \mathbf{H}^{[kj]}$, where α is the path-loss exponent and d_{kj} is the propagation distance. Let $\mathbf{V}^{[j]} = [\mathbf{v}^{[j]}_1 \cdots \mathbf{v}^{[j]}_d]$ and $\mathbf{R}^{[k]} = [\mathbf{r}^{[k]}_1 \cdots \mathbf{r}^{[k]}_d]$ denote $M \times d$ precoder at transmitter j and receive filter at receiver k , where $\|\mathbf{v}^{[j]}_i\|^2 = \|\mathbf{r}^{[k]}_i\|^2 = 1, \forall i$. Then, the signal vector received at receiver k for i -th data stream can be written as

$$\mathbf{y}_i^{[k]} = \sqrt{\frac{P}{d}} d_{kk}^{-\alpha/2} \mathbf{H}^{[kk]} \mathbf{v}_i^{[k]} s_i^k + \sum_{l \neq i} \sqrt{\frac{P}{d}} d_{kk}^{-\alpha/2} \mathbf{H}^{[kk]} \mathbf{v}_l^{[k]} s_l^k + \sum_{j \neq k} \sqrt{\frac{P}{d}} d_{kj}^{-\alpha/2} \mathbf{H}^{[kj]} \mathbf{V}^{[j]} \mathbf{s}^j + \mathbf{n}_k \quad (1)$$

where $\mathbf{s}^k = [s_1^k \cdots s_d^k]^T$ denotes the data symbols with $s_i^k = \mathcal{CN}(0, 1)$, P is the transmission power and \mathbf{n}_k is additive white Gaussian noise (AWGN) vector with the covariance matrix \mathbf{I}_M .

Throughout this paper, we consider FDD system and assume that each receiver has perfect knowledge of the fading coefficients $\{\mathbf{H}^{[km]}\}_{m=1}^K$. For the case of perfect CSIT, all interfering signals at each receiver can be fully eliminated by using IA precoders and ZF receive filters so that the achievable throughput is given by

$$R_{\text{perfect}} = \sum_{k=1}^K \sum_{i=1}^d \log_2 \left(1 + P d_{kk}^{-\alpha} \left| \mathbf{r}_i^{[k]\dagger} \mathbf{H}^{[kk]} \mathbf{v}_i^{[k]} \right|^2 \right). \quad (2)$$

A. Closed-form IA Precoder

In [8], Bresler *et al.* prove that IA over MIMO constant channel is feasible if and only if the number of antennas satisfies $M \geq d(K+1)/2$ under the symmetric square case where all transmitters and receiver are equipped with the same number of antennas. However, the transceiver designs of IA satisfying above feasibility condition are not explicitly addressed except for $K = 3$ and global CSI is required at all transmit sides for the computation of IA precoders [1]. In [27], the closed-form IA solution for a single data transmission has been proposed under the constraint of $K = M + 1$. The main principle of closed-form IA is that the $k+1$ -th and $k+2$ -th IA precoders are designed for aligning the interfering signals from transmitter $k+1$ and $k+2$ in the same subspace at receiver k . Then, $K-1$ dimensional interference vectors lie in $K-2 = M-1$ dimensional subspace at each receiver, which allows one dimensional interference-free link for each receiver. Extending the closed-form IA solution for a single data stream

to the case of multiple data streams transmission, we obtain the IA conditions as follows.

$$\begin{aligned}
\text{span}(\mathbf{H}^{[12]}\mathbf{V}^{[2]}) &= \text{span}(\mathbf{H}^{[13]}\mathbf{V}^{[3]}) && \text{at receiver 1} \\
\text{span}(\mathbf{H}^{[23]}\mathbf{V}^{[3]}) &= \text{span}(\mathbf{H}^{[24]}\mathbf{V}^{[4]}) && \text{at receiver 2} \\
&\vdots && \\
\text{span}(\mathbf{H}^{[K-1K]}\mathbf{V}^{[K]}) &= \text{span}(\mathbf{H}^{[K-11]}\mathbf{V}^{[1]}) && \text{at receiver } K-1 \\
\text{span}(\mathbf{H}^{[K1]}\mathbf{V}^{[1]}) &= \text{span}(\mathbf{H}^{[K2]}\mathbf{V}^{[2]}) && \text{at receiver } K
\end{aligned} \tag{3}$$

where $\text{span}(\mathbf{A})$ denotes the vector space that spanned by the columns of \mathbf{A} . Note that $\text{span}(\mathbf{H}^{[k-1k]}\mathbf{V}^{[k]}) = \text{span}(\mathbf{H}^{[k-1k+1]}\mathbf{V}^{[k+1]}) \Rightarrow \text{span}(\mathbf{V}^{[k+1]}) = \text{span}\left((\mathbf{H}^{[k-1k+1]})^{-1}\mathbf{H}^{[k-1k]}\mathbf{V}^{[k]}\right)$ and $\{\text{span}(\mathbf{V}^{[k]})\}_{k=1}^K$ are concatenated with each other. From (3), IA precoders are computed by

$$\begin{aligned}
\mathbf{V}^{[1]} &= d \text{ eigenvectors of } \left((\mathbf{H}^{[K-11]})^{-1}\mathbf{H}^{[K-1K]}\dots(\mathbf{H}^{[13]})^{-1}\mathbf{H}^{[12]}(\mathbf{H}^{[K2]})^{-1}\mathbf{H}^{[K1]}\right) \\
\mathbf{V}^{[2]} &= (\mathbf{H}^{[K2]})^{-1}\mathbf{H}^{[K1]}\mathbf{V}^{[1]} \\
\mathbf{V}^{[3]} &= (\mathbf{H}^{[13]})^{-1}\mathbf{H}^{[12]}\mathbf{V}^{[2]} \\
&\vdots \\
\mathbf{V}^{[K]} &= (\mathbf{H}^{[K-2K]})^{-1}\mathbf{H}^{[K-2K-1]}\mathbf{V}^{[K-1]}
\end{aligned} \tag{4}$$

and then each column of the precoders is normalized to have unit norm. From the design of IA precoders in (4), total $(K-1)d$ dimensional interferers are shrunk into the $(K-2)d$ dimensional subspace at each receiver. Since the desired signals occupy d dimensions of the M dimensional receive space, the number of antennas should satisfy at least $M = (K-2)d + d$ for the proposed IA design. Given these antenna configurations, we can achieve d DoF for each user under the design of ZF receive filter.

B. Feedback Structure

In the existing IA literature, the design of feedback topology is not explicitly addressed. Existing works [15],[16] commonly assume that each receiver feeds back the estimated CSI to all transmitters. This corresponds to a *full-feedback topology* as illustrated in Fig. 1. We consider the full-feedback topology as the conventional feedback approach for achieving IA and measure its efficiency as the CSI overhead

$$N = \sum_{m,k \in \{1,2,\dots,K\}} \left(N_{\text{TR}}^{[mk]} + N_{\text{RT}}^{[mk]}\right) \tag{5}$$

where $N_{\text{TR}}^{[mk]}$ denotes the number of complex CSI coefficients sent from receiver k to transmitter m and $N_{\text{RT}}^{[mk]}$ from transmitter k to receiver m . In the full-feedback topology, each receiver feeds back all interfering channels that consist of $(K-1)M^2$ complex coefficients to all transmitters. Since each of all receivers feed back the same amount of CSI coefficients to all transmitters, total CSI overhead is given by

$$N_{\text{FF}} = K^2(K-1)M^2 \tag{6}$$

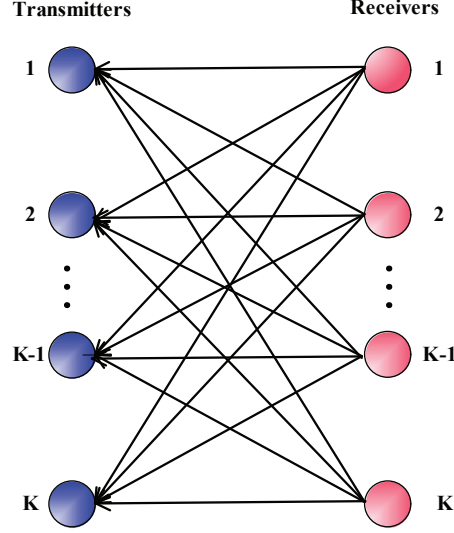


Fig. 1. Full-feedback topology for achieving IA

where the overhead N_{FF} increases as $\mathcal{O}(K^3 M^2)$ whereas the network throughput grows linearly with K only. Thus the CSI overhead is quickly overweighted to the network throughput for large K .

III. CSI-FEEDBACK TOPOLOGIES

The conventional IA technique potentially leads to unacceptable CSI-feedback overhead given the existence of many feedback links. To reduce the requirement of global CSI, the numerical methods have been proposed in the iterative algorithm which progressively update the transmit/receive filters by using local channel knowledge at each node [10]. This iterative method achieves a full DoF under the feasibility condition $M \geq d(K+1)/2$, but it results in a slow convergence rate that causes the huge amount of system overhead. In this section, we propose three practical CSI feedback topologies, namely the *CSI-exchange*, *modified CSI-exchange* and *star feedback* topologies. The design of proposed feedback topologies build upon the closed-form IA solution in (4) and the efficiency is measured by the metric in (5). To implement the proposed feedback topologies, we make the following assumptions:

- 1) CSI can be exchanged in both direction between a transmitter and receiver through feedforward/feedback channels. The effect of quantization error due to the limited feedforward/feedback channels is discussed in next section.
- 2) In order to share CSI between receivers, we assume that each receiver is directly connected with others. This connectivity is feasible for the receivers who are linked with local area networks such as Wi-Fi [25], [26]. Also, the coordinated multi-point(CoMP) system which provides the high capacity backhaul links between base stations can be applicable for this scenario.

A. CSI-Exchange Topology

Consider $K = 4$ user interference channel with $M = 3d$. From (4), the IA precoders $\mathbf{V}^{[1]}, \mathbf{V}^{[2]}, \mathbf{V}^{[3]}$ and $\mathbf{V}^{[4]}$ are represented as

$$\begin{aligned}\mathbf{V}^{[1]} &= d \text{ eigenvectors of } \left((\mathbf{H}^{[31]})^{-1} \mathbf{H}^{[34]} (\mathbf{H}^{[24]})^{-1} \mathbf{H}^{[23]} (\mathbf{H}^{[13]})^{-1} \mathbf{H}^{[12]} (\mathbf{H}^{[42]})^{-1} \mathbf{H}^{[41]} \right) \\ \mathbf{V}^{[2]} &= (\mathbf{H}^{[42]})^{-1} \mathbf{H}^{[41]} \mathbf{V}^{[1]} \\ \mathbf{V}^{[3]} &= (\mathbf{H}^{[13]})^{-1} \mathbf{H}^{[12]} \mathbf{V}^{[2]} \\ \mathbf{V}^{[4]} &= (\mathbf{H}^{[24]})^{-1} \mathbf{H}^{[23]} \mathbf{V}^{[3]}\end{aligned}\tag{7}$$

and normalized to unit norm at each column. As shown in (7), the k -th precoder $\mathbf{V}^{[k]}$ is sequentially determined by the product of pre-determined $\mathbf{V}^{[k-1]}$ and the estimated channel matrix $(\mathbf{H}^{[k-2k]})^{-1} \mathbf{H}^{[k-2k-1]}$ at receiver $k-2$. These properties motivate the design of sequential CSI-exchange topology in Algorithm 1, which only exchanges precoding matrices between transmitters and receivers after the computation of $\mathbf{V}^{[1]}$. Fig. 2 (a) illustrates CSI-exchange topology for $K = 4$ user interference channel and its procedure, $R_3 \xrightarrow{\mathbf{V}^{[1]}} T_1 \xrightarrow{\mathbf{V}^{[1]}} R_4 \xrightarrow{\mathbf{V}^{[2]}} T_2 \xrightarrow{\mathbf{V}^{[2]}} R_1 \xrightarrow{\mathbf{V}^{[3]}} T_3 \xrightarrow{\mathbf{V}^{[3]}} R_2 \xrightarrow{\mathbf{V}^{[4]}} T_4$, where T_m and R_n represent transmitter m and receiver n , respectively. In Algorithm 1, all receivers transmit CSI of the product channel matrices to receiver $K-1$, which comprises $(K-1)M^2$ complex-valued coefficients. After computing the precoder $\mathbf{V}^{[1]}$, receiver $K-1$ feeds back the Md complex-valued $\mathbf{V}^{[1]}$ to transmitter 1. Then, each precoder is determined by iterative exchange of precoders between transmitters and interfered receivers. In each round of exchange, the number of nonzero coefficients of feedforward/feedback becomes $2Md$. Therefore, total CSI overhead in the CSI-exchange topology requires

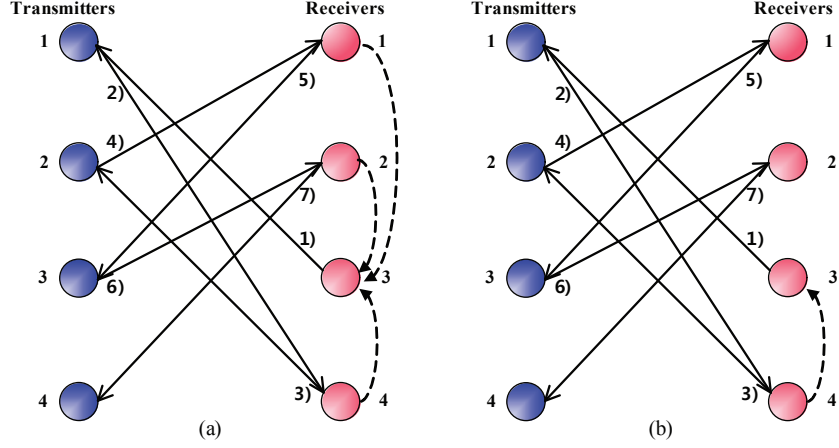
$$N_{\text{EX}} = (K-1)M^2 + (2K-1)Md.\tag{8}$$

From (8), the proposed topology provides much less sum overhead for achieving IA, namely on the order of KM^2 , whereas the conventional feedback approach requires the feedback overhead of K^3M^2 order.

B. Modified CSI-Exchange Topology ($K \geq 4$)

In CSI-exchange topology, $\mathbf{V}^{[1]}$ is solved by the eigenvalue problem that incorporates the channel matrices of all interfering links which causes a significant overhead for the case of many links or antennas. To reduce the CSI overhead for the computation of $\mathbf{V}^{[1]}$, we design two interferers from transmitter 1 and 2 are aligned in the same subspace at receiver $K-1$ and K as following conditions:

$$\begin{aligned}\text{span}(\mathbf{H}^{[K-11]} \mathbf{V}^{[1]}) &= \text{span}(\mathbf{H}^{[K-12]} \mathbf{V}^{[2]}) \quad \text{at receiver } K-1 \\ \text{span}(\mathbf{H}^{[K1]} \mathbf{V}^{[1]}) &= \text{span}(\mathbf{H}^{[K2]} \mathbf{V}^{[2]}) \quad \text{at receiver } K\end{aligned}\tag{9}$$

Fig. 2. CSI-exchange topologies for achieving IA with $K=4$ and $M=3$ **Algorithm 1:** CSI-exchange topology

Let denote that $\bar{k} = \text{mod}(k, K) + 1$ and $\tilde{k} = \text{mod}(K + (k - 2), K) + 1$, where $\text{mod}(n, k)$ represents the modulo operation.

1. Computation of $\mathbf{V}^{[1]}$

Receiver k , ($k \neq K - 1$), transmits the corresponding interference channel $(\mathbf{H}^{[k \bar{k}+1]})^{-1} \mathbf{H}^{[k \bar{k}]}$ to receiver $K - 1$.

Then, receiver $K - 1$ computes $\mathbf{V}^{[1]}$ as d eigenvectors of $(\mathbf{H}^{[K-11]})^{-1} \mathbf{H}^{[K-1K]} \dots (\mathbf{H}^{[13]})^{-1} \mathbf{H}^{[12]} (\mathbf{H}^{[K2]})^{-1} \mathbf{H}^{[K1]}$ and feeds it back to transmitter 1.

2. Exchange of precoders $\mathbf{V}^{[1]}, \dots, \mathbf{V}^{[K]}$

for $k=1:K - 1$ **do**

 Transmitter k forwards $\mathbf{V}^{[k]}$ to receiver \tilde{k} . Then, receiver \tilde{k} calculates $\mathbf{V}^{[k+1]}$ and feeds back to transmitter $k + 1$.

Substituting (9) with last two conditions in (3), IA precoders $\mathbf{V}^{[1]}, \mathbf{V}^{[2]}, \dots, \mathbf{V}^{[K]}$ are modified as

$$\begin{aligned}
 \mathbf{V}^{[1]} &= d \text{ eigenvectors of } \left((\mathbf{H}^{[K-11]})^{-1} \mathbf{H}^{[K-12]} (\mathbf{H}^{[K2]})^{-1} \mathbf{H}^{[K1]} \right) \\
 \mathbf{V}^{[2]} &= (\mathbf{H}^{[K2]})^{-1} \mathbf{H}^{[K1]} \mathbf{V}^{[1]} \\
 \mathbf{V}^{[3]} &= (\mathbf{H}^{[13]})^{-1} \mathbf{H}^{[12]} \mathbf{V}^{[2]} \\
 &\vdots \\
 \mathbf{V}^{[K]} &= (\mathbf{H}^{[K-2K]})^{-1} \mathbf{H}^{[K-2K-1]} \mathbf{V}^{[K-1]}.
 \end{aligned} \tag{10}$$

Based on (10), the modified CSI-exchange topology is designed by replacing step 1 in Algorithm 1 with following statement. Fig. 2 (b) illustrates the procedure of modified CSI-exchange topology for $K = 4$

interference channels.

Computation of $\mathbf{V}^{[1]}$: Receiver K forwards the matrix $(\mathbf{H}^{[K2]})^{-1} \mathbf{H}^{[K1]}$ to receiver $K - 1$. Then, receiver $K - 1$ computes $\mathbf{V}^{[1]}$ as d eigenvectors of $(\mathbf{H}^{[K-11]})^{-1} \mathbf{H}^{[K-12]} (\mathbf{H}^{[K2]})^{-1} \mathbf{H}^{[K1]}$ and feeds it back to the transmitter 1.

For the computation of $\mathbf{V}^{[1]}$, CSI-exchange topology requires the $(K - 1)M^2$ complex-valued feedback overhead. In contrast, the modified CSI-exchange topology computes $\mathbf{V}^{[1]}$ by using the feedback of $(\mathbf{H}^{[K2]})^{-1} \mathbf{H}^{[K1]}$ which consists of M^2 complex-valued coefficients. Therefore, CSI overhead in the modified CSI-exchange topology is given as follow.

$$N_{\text{MEX}} = M^2 + (2K - 1)Md. \quad (11)$$

Comparing (11) with (8), both CSI-exchange topologies have the same sum overhead for the exchange of precoders between transmitters and receivers, scaling with $\mathcal{O}(KM)$. However, the product channel matrices for computing $\mathbf{V}^{[1]}$ in modified CSI-exchange topology requires constant M^2 overhead in any K user cases while that of CSI-exchange topology increases with $\mathcal{O}(KM^2)$.

C. Star Feedback Topology

While the CSI-exchange topologies degrade the amount of feedback overhead compared with the full-feedback topology, such two topologies commonly incur $2K - 1$ iterations caused by the procedure of multiple-hop feedforward/feedback between the transmitter and the receiver. As the number of iterations is increased, a full DoF in K -user interference channel can not be achievable since it causes the time delay of transmission that results in significant interference misalignment for fast fading. To address these issues, we propose the star feedback topology illustrated in Fig. 3 and describe details in Algorithm 2. The star feedback topology comprises an agent, called the *CSI base station* (CSI-BS) which collects CSI from all receivers, computes all precoders using IA condition in (3) and sends them back to corresponding transmitters. Therefore, star feedback topology can be structured by two-hop feedback framework: (i) the feedback channels from all receivers to CSI-BS that gather the set of interfering matrices which comprise KM^2 complex-valued coefficients and (ii) the feedback channels that CSI-BS transmits a precoder of Md coefficients to each of K transmitters. Combining the overhead in (i) and (ii), we obtain CSI overhead in the star feedback topology as

$$N_{\text{SF}} = (M^2 + Md)K. \quad (12)$$

Star feedback topology requires only two time slots for computation of IA precoders in any number of user K . Therefore, it is robust against channel variations due to the fast fading while CSI exchange is

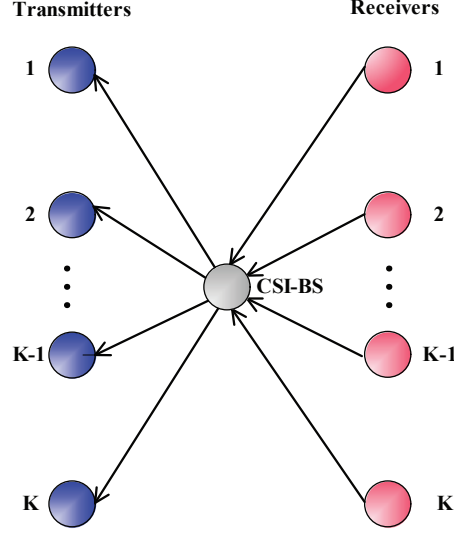


Fig. 3. Star feedback topology for achieving IA

Algorithm 2: Star feedback topology

- 1. Computation of $\mathbf{V}^{[1]}, \dots, \mathbf{V}^{[K]}$** : The CSI-BS collects $(\mathbf{H}^{[K-11]})^{-1} \mathbf{H}^{[K-1K]}, \dots, (\mathbf{H}^{[13]})^{-1} \mathbf{H}^{[12]}$ and $(\mathbf{H}^{[K2]})^{-1} \mathbf{H}^{[K1]}$ from the corresponding receivers and computes $\mathbf{V}^{[1]}, \dots, \mathbf{V}^{[K]}$ with the collected set of CSI.
- 3. Broadcasting $\mathbf{V}^{[1]}, \dots, \mathbf{V}^{[K]}$** : CSI-BS transmits $\mathbf{V}^{[k]}$ to the corresponding transmitter k , $\forall k$.

affected by $2K - 1$ slot delay for implementation. Even though the feedforward links are not required in the star feedback topology, CSI-BS that connects all pairs of transmitter-receiver should be implemented as the additional costs. In addition, the feedback overhead is increased with $\mathcal{O}(KM^2)$ which is larger than $\mathcal{O}(KM)$ in modified CSI exchange topology. Fig. 4 compares the CSI overhead of two proposed feedback topologies for $d = 1$ scenarios. We figure out that a full-feedback topology provides dramatic CSI overhead compared with the proposed feedback topologies, while star feedback topology shows slightly larger overhead than that of modified CSI-exchange scheme.

IV. EFFECT OF CSI-FEEDBACK QUANTIZATION

The proposed feedback topologies are designed under the assumption of perfect CSI exchange in the preceding section. However, in practical communication systems, CSI is quantized at each receiver and sent back to the corresponding transmitter through a finite-rate feedback constraints which causes the performance degradation due to the residual interference at receive sides. In this section, we analyze the throughput loss in the proposed feedback topologies as the performance degradation due to the limited

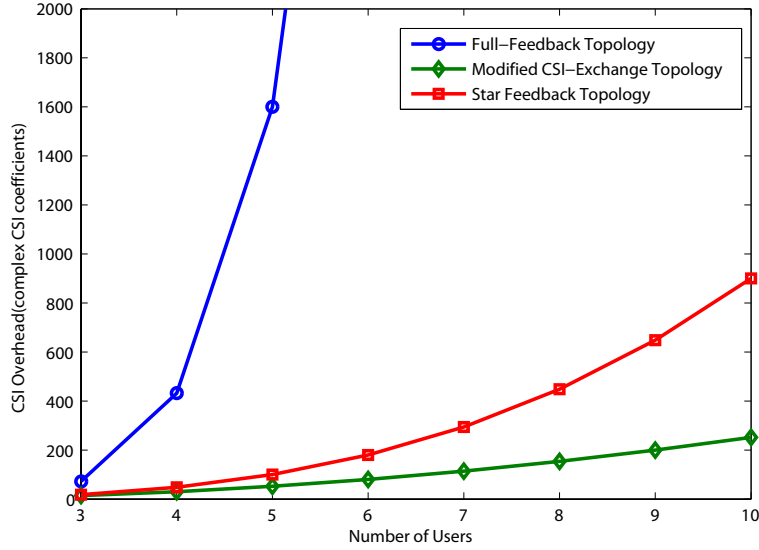


Fig. 4. Comparison of feedback CSI overhead in the proposed topologies

feedback channels [24]. The RVQ is used for CSI quantization and a single data transmission $d = 1$ is considered for analytical simplicity.

A. Quantization Error in Limited Feedback

Prior to deriving the throughput loss, we quantify the quantization error with RVQ using the distortion measure. Let denote a $M \times 1$ beamformer $\mathbf{v}^{[k]}$ at transmitter k , satisfying $\|\mathbf{v}^{[k]}\|^2 = 1$ and the quantization codebook \mathcal{W} known to both transmitters and receivers. Given B_k feedback-bits, the codebook \mathcal{W} consists of 2^{B_k} independently selected random vectors from the isotropic distribution on the M dimensional complex unit sphere, where $\mathcal{W} = \{\hat{\mathbf{v}}_1, \dots, \hat{\mathbf{v}}_{2^{B_k}}\}$. The quantized beamformer $\hat{\mathbf{v}}^{[k]}$ is selected by the minimal chordal distance metric:

$$\hat{\mathbf{v}}^{[k]} = \arg \min_{\hat{\mathbf{v}}_i \in \mathcal{W}} d^2(\mathbf{v}^{[k]}, \hat{\mathbf{v}}_i),$$

where $d(\mathbf{v}^{[k]}, \hat{\mathbf{v}}_i) = \sin \theta = \sqrt{1 - |\mathbf{v}^{[k]\dagger} \hat{\mathbf{v}}_i|^2}$ and θ denotes the principle angle between $\mathbf{v}^{[k]}$ and $\hat{\mathbf{v}}^{[k]}$. Using the quantized beamformer $\hat{\mathbf{v}}^{[k]}$, we model the $\mathbf{v}^{[k]}$ as

$$\mathbf{v}^{[k]} = \hat{\mathbf{v}}^{[k]} + \Delta \mathbf{v}^{[k]}, \quad (13)$$

where $\Delta \mathbf{v}^{[k]}$ represents the quantization error of $\mathbf{v}^{[k]}$.

In following lemma, we characterize the quantization error as a function of the number of feedback-bits and antennas, which is used for the analysis of residual interference in the proposed IA topologies.

Lemma 1. *The expected squared norm of $\Delta \mathbf{v}^{[k]}$ over \mathcal{W} is bounded as*

$$E_{\mathcal{W}} \left[\left\| \Delta \mathbf{v}^{[k]} \right\|^2 \right] \leq \bar{\Gamma}(M) \cdot 2^{-\frac{B_k}{M-1}} \quad (14)$$

where B_k denotes feedback-bits for quantizing $\mathbf{v}^{[k]}$ and $\bar{\Gamma}(M) = \frac{4\Gamma(\frac{1}{M-1})}{M-1}$.

Proof: See Appendix A. ■

From the result of Lemma 1, we normalize the quantization error and then rewrite (13) as

$$\mathbf{v}^{[k]} = \hat{\mathbf{v}}^{[k]} + \sigma_k \Delta \bar{\mathbf{v}}^{[k]} \quad (15)$$

where $E_{\mathcal{W}} \left[\left\| \Delta \bar{\mathbf{v}}^{[k]} \right\|^2 \right] = 1$ and $\sigma_k^2 \leq \bar{\Gamma}(M) \cdot 2^{-\frac{B_k}{M-1}}$.

B. Throughput Loss Analysis

Let denote $\hat{\mathbf{v}}^{[j]}$ and $\hat{\mathbf{r}}^{[k]}$ as the transmit beamformer and receive filter calculated in the presence of CSI quantization errors. Then, we write the residual interference power at receiver k as

$$\hat{I}^{[k]} = \sum_{k \neq j} P d_{kj}^{-\alpha} \left| \hat{\mathbf{r}}^{[k]\dagger} \mathbf{H}^{[kj]} \hat{\mathbf{v}}^{[j]} \right|^2 \quad (16)$$

and the sum throughput as

$$R_{\text{limited}} = \sum_{k=1}^K \log_2 \left(1 + \frac{P d_{kk}^{-\alpha} \left| \hat{\mathbf{r}}^{[k]\dagger} \mathbf{H}^{[kk]} \hat{\mathbf{v}}^{[k]} \right|^2}{\hat{I}^{[k]} + 1} \right). \quad (17)$$

In this subsection, we derive the throughput loss ΔR_{sum} , which represents the difference between the sum throughput by perfect CSIT-based IA and limited feedback-based IA: $\Delta R_{\text{sum}} = E_{\mathbf{H}, \mathcal{W}} [R_{\text{perfect}} - R_{\text{limited}}]$.

From (2) and (17), the throughput loss is bounded as

$$\begin{aligned} \Delta R_{\text{sum}} &= E_{\mathbf{H}} \left[\sum_{k=1}^K \log_2 \left(1 + P d_{kk}^{-\alpha} \left| \mathbf{r}^{[k]\dagger} \mathbf{H}^{[kk]} \mathbf{v}^{[k]} \right|^2 \right) \right] - E_{\mathbf{H}, \mathcal{W}} \left[\sum_{k=1}^K \log_2 \left(1 + \frac{P d_{kk}^{-\alpha} \left| \hat{\mathbf{r}}^{[k]\dagger} \mathbf{H}^{[kk]} \hat{\mathbf{v}}^{[k]} \right|^2}{1 + \hat{I}^{[k]}} \right) \right] \\ &= E_{\mathbf{H}} \left[\sum_{k=1}^K \log_2 \left(1 + P d_{kk}^{-\alpha} \left| \mathbf{r}^{[k]\dagger} \mathbf{H}^{[kk]} \mathbf{v}^{[k]} \right|^2 \right) \right] \\ &\quad - E_{\mathbf{H}, \mathcal{W}} \left[\sum_{k=1}^K \log_2 \left(1 + \hat{I}^{[k]} + P d_{kk}^{-\alpha} \left| \hat{\mathbf{r}}^{[k]\dagger} \mathbf{H}^{[kk]} \hat{\mathbf{v}}^{[k]} \right|^2 \right) \right] + E_{\mathbf{H}, \mathcal{W}} \left[\sum_{k=1}^K \log_2 \left(1 + \hat{I}^{[k]} \right) \right] \\ &\leq E_{\mathbf{H}} \left[\sum_{k=1}^K \log_2 \left(1 + P d_{kk}^{-\alpha} \left| \mathbf{r}^{[k]\dagger} \mathbf{H}^{[kk]} \mathbf{v}^{[k]} \right|^2 \right) \right] \\ &\quad - E_{\mathbf{H}, \mathcal{W}} \left[\sum_{k=1}^K \log_2 \left(1 + P d_{kk}^{-\alpha} \left| \hat{\mathbf{r}}^{[k]\dagger} \mathbf{H}^{[kk]} \hat{\mathbf{v}}^{[k]} \right|^2 \right) \right] + E_{\mathbf{H}, \mathcal{W}} \left[\sum_{k=1}^K \log_2 \left(1 + \hat{I}^{[k]} \right) \right] \\ &\stackrel{(a)}{=} E_{\mathbf{H}, \mathcal{W}} \left[\sum_{k=1}^K \log_2 \left(1 + \hat{I}^{[k]} \right) \right] \\ &\stackrel{(b)}{\leq} E_{\mathbf{H}, \mathcal{W}} \left[K \cdot \log_2 \left(1 + \frac{1}{K} \sum_{k=1}^K \hat{I}^{[k]} \right) \right] \end{aligned} \quad (18)$$

where (a) follows the fact that $\mathbf{v}^{[k]}$, $\mathbf{r}^{[k]}$, $\hat{\mathbf{v}}^{[k]}$ and $\hat{\mathbf{r}}^{[k]}$ are independently distributed in $\mathcal{C}^{M \times 1}$ and (b) uses the characteristic of concave function, $\log(x)$. Applying Jensen's inequality to the upper-bound in (18), the throughput loss is upper-bounded by

$$\Delta R_{\text{sum}} \leq K \cdot \log_2 \left(1 + \frac{1}{K} E_{\mathbf{H}, \mathcal{W}} \left[\sum_{k=1}^K \hat{I}^{[k]} \right] \right). \quad (19)$$

This bound explains that the throughput loss is logarithmically increased with the sum of residual interference. To minimize the throughput loss due to the quantization error, we analyze the residual interference at each receiver and regulate it by utilizing a variable feedback-bits allocation schemes in following sections.

C. Residual Interference Relative to Quantization Error

1) *Modified CSI-Exchange Topology*: Under the finite-rate feedforward/feedback channels between transmitters and receivers, we analyze the residual interference in modified CSI-exchange topology that consists of two types of CSI exchange links: (i) exchange of the channel matrix between receiver $K - 1$ and K and (ii) sequential exchange of quantized beamformer between transmitters and receivers through feedforward/feedback links. For tractability, we assume that receiver $K - 1$ and K are located in local areas and linked with high-capacity Wi-Fi links [25], [26]. This connectivity is feasible in the integrated heterogeneous network (e.g., Wi-Fi / cellular) which provides user cooperation in short-range area so that the perfect CSI sharing is allowed to both receivers [31]. Then, receiver $K - 1$ computes $\mathbf{v}^{[1]}$ and feeds back the quantized beamformer $\hat{\mathbf{v}}^{[1]}$ to transmitter 1, chosen according to :

$$\hat{\mathbf{v}}^{[1]} = \arg \min_{\hat{\mathbf{v}}_i \in \mathcal{C}} d^2(\mathbf{v}^{[1]}, \hat{\mathbf{v}}_i).$$

Using (15), we represent the $\hat{\mathbf{v}}^{[1]}$ as

$$\hat{\mathbf{v}}^{[1]} = \mathbf{v}^{[1]} - \sigma_1 \Delta \bar{\mathbf{v}}^{[1]} \quad (20)$$

where $\sigma_1^2 = \bar{\Gamma}(M) 2^{-\frac{B_1}{M-1}}$ and $E_{\mathcal{W}} \left[\|\Delta \bar{\mathbf{v}}^{[1]}\|^2 \right] = 1$. Similarly, receiver K designs $\mathbf{v}^{[2]}$ and feeds it back to transmitter 2 using the quantized beamformer $\hat{\mathbf{v}}^{[2]}$,

$$\hat{\mathbf{v}}^{[2]} = \mathbf{v}^{[2]} - \sigma_2 \Delta \bar{\mathbf{v}}^{[2]} \quad (21)$$

where $\sigma_2^2 = \bar{\Gamma}(M) 2^{-\frac{B_2}{M-1}}$ and $E_{\mathcal{W}} \left[\|\Delta \bar{\mathbf{v}}^{[2]}\|^2 \right] = 1$. For $\hat{\mathbf{v}}^{[k]}$, $k = 3, \dots, K$, receiver $k - 2$ sequentially designs $\bar{\mathbf{v}}^{[k]}$ in the subspace of $(\mathbf{H}^{[k-2k]})^{-1} \mathbf{H}^{[k-2k-1]} \hat{\mathbf{v}}^{[k-1]}$ and feeds back the quantized $\hat{\mathbf{v}}^{[k]}$ to transmitter k . Then, $\hat{\mathbf{v}}^{[k]}$ can be represented as

$$\hat{\mathbf{v}}^{[k]} = \bar{\mathbf{v}}^{[k]} - \sigma_k \Delta \bar{\mathbf{v}}^{[k]}, \quad (22)$$

where $\sigma_k^2 = 2^{-\frac{B_k}{M-1}}$ and $E_{\mathcal{W}} \left[\|\Delta \bar{\mathbf{v}}^{[k]}\|^2 \right] = 1$. From (20), (21) and (22), we derive the upper-bound of residual interference averaged over all random choices of codebooks in following Proposition.

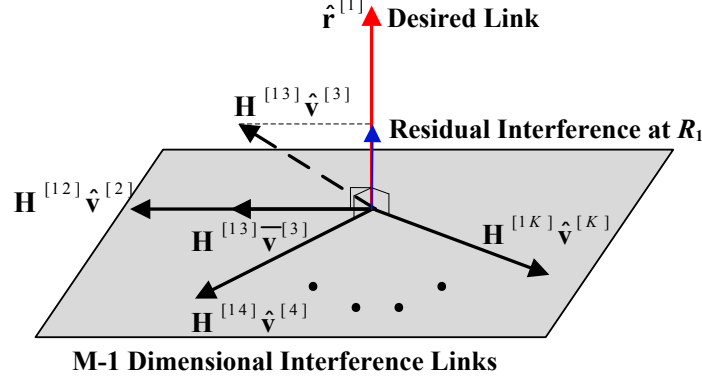


Fig. 5. Residual interference at receiver 1 in the modified CSI-exchange topology

Proposition 1. *In modified CSI-feedback topology, the upper-bound of expected residual interference at each receiver is represented as ¹*

$$\begin{cases} E_{\mathcal{W}} \left(\hat{I}^{[k]} \right) & \leq P d_{kk+2}^{-\alpha} \sigma_{k+2}^2 \lambda_{\max}^{[kk+2]}, \quad k = 1, \dots, K-2 \\ E_{\mathcal{W}} \left(\hat{I}^{[K-1]} \right) & \leq P d_{K-12}^{-\alpha} \sigma_1^2 \lambda_{\max}^{[K-11]} + P d_{K-12}^{-\alpha} \sigma_2^2 \lambda_{\max}^{[K-12]} \\ E_{\mathcal{W}} \left(\hat{I}^{[K]} \right) & \leq P d_{K1}^{-\alpha} \sigma_2^2 \lambda_{\max}^{[K2]} + P d_{K1}^{-\alpha} \sigma_1^2 \lambda_{\max}^{[K1]} \end{cases} \quad (23)$$

in given feedback bits $\{B_k\}_{k=1}^K$ and channel realization $\{\mathbf{H}^{[jk]}\}_{j,k=1}^K$, where $\lambda_{\max}^{[ij]}$ is a maximum eigenvalue of $\mathbf{H}^{[ij]}(\mathbf{H}^{[ij]})^H$.

Proof: See Appendix B. ■

In Proposition 1, the expected residual interference in modified CSI-exchange topology is characterized as a function of the feedback-bits, the gains of interfering fading channel and path-loss between the pairs of transmitter-receiver. Since $\mathbf{v}^{[1]}$ and $\mathbf{v}^{[2]}$ are designed based on the IA condition (9), both quantized $\hat{\mathbf{v}}^{[1]}$ and $\hat{\mathbf{v}}^{[2]}$ affect the residual interference at receiver $K-1$ and K in (23). However, other receiver k sequentially designs $\hat{\mathbf{v}}^{[k+2]}$ based on the pre-determined $\hat{\mathbf{v}}^{[k+1]}$ so that the interference at receiver k is only affected by the quantization error of $\hat{\mathbf{v}}^{[k+2]}$, respectively. Fig. 5 depicts the residual interference at receiver 1 in modified CSI-exchange topology, as an example.

2) *Star Feedback Topology:* In a star feedback topology, we assume that all receivers are connected to CSI-BS with high capacity backhaul links which allows CSI-BS to acquire full knowledge of CSI estimated at each receiver. Then, CSI-BS can compute $\mathbf{v}^{[1]}, \mathbf{v}^{[2]}, \dots, \mathbf{v}^{[K]}$ using (4) and forwards them to the corresponding transmitters for achieving IA. However, we consider the B_k bits are allocated to the feedback channel from CSI-BS to transmitter k , which incurs the residual interference at each receiver.

¹To derive the residual interference, a full knowledge of $\{\hat{\mathbf{v}}^{[k]} : 1 \leq k \leq K\}$ is assumed at each receiver.

To analyze the effect of limited feedback channel on the residual interference, we model the quantized $\hat{\mathbf{v}}^{[k]}$ as

$$\hat{\mathbf{v}}^{[k]} = \mathbf{v}^{[k]} - \sigma_k \Delta \bar{\mathbf{v}}^{[k]} \quad (24)$$

where $\sigma_k^2 = \bar{\Gamma}(M) 2^{-\frac{B_k}{M-1}}$ and $E_{\mathcal{W}} [\|\Delta \bar{\mathbf{v}}^{[k]}\|^2] = 1, \forall k$. Using (24), the upper-bound of expected residual interference is derived in following proposition.

Proposition 2. *In star feedback topology, the upper-bound of expected residual interference at each receiver is represented as*

$$\begin{cases} E_{\mathcal{W}} (\hat{I}^{[k]}) & \leq P d_{kk+2}^{-\alpha} \sigma_{k+1}^2 \lambda_{\max}^{[kk+1]} + P d_{kk+2}^{-\alpha} \sigma_{k+2}^2 \lambda_{\max}^{[kk+2]}, \quad k = 1, \dots, K-2 \\ E_{\mathcal{W}} (\hat{I}^{[K-1]}) & \leq P d_{K-11}^{-\alpha} \sigma_K^2 \lambda_{\max}^{[K-1K]} + P d_{K-11}^{-\alpha} \sigma_1^2 \lambda_{\max}^{[K-11]} \\ E_{\mathcal{W}} (\hat{I}^{[K]}) & \leq P d_{K2}^{-\alpha} \sigma_1^2 \lambda_{\max}^{[K1]} + P d_{K2}^{-\alpha} \sigma_2^2 \lambda_{\max}^{[K2]} \end{cases} \quad (25)$$

in given feedback bits $\{B_k\}_{k=1}^K$ and channel realization $\{\mathbf{H}^{[jk]}\}_{j,k=1}^K$.

Proof: See Appendix C. ■

In Proposition 2, the residual interference at receiver k is generated by the misalignment between interference from transmitter $k+1$ and $k+2$. The upper-bound of residual interference at each receiver consists of the number of feedback-bits, the interfering channel gain and path-loss between the pairs of transmitter-receiver.

V. FEEDBACK-BIT ALLOCATION STRATEGIES

In cooperative base-station systems, adaptive feedback bit partitioning between desired and interfering channel at each receiver has been proposed to minimize the mean loss of sum throughput in [28], [29]. This motivates us to design the dynamic feedback-bit allocation strategies that adaptively distributes the number of feedback-bits to each pair of link for minimizing the throughput loss. To implement the feedback-bits allocation scheme, we consider the centralized bit controller which gathers channel gains from all receivers and computes the number of feedback-bits for each receiver. Fig. 6 depicts the structure of dynamic feedback-bit allocation in K -user interference channels under the constraints of total B_T feedback-bits.

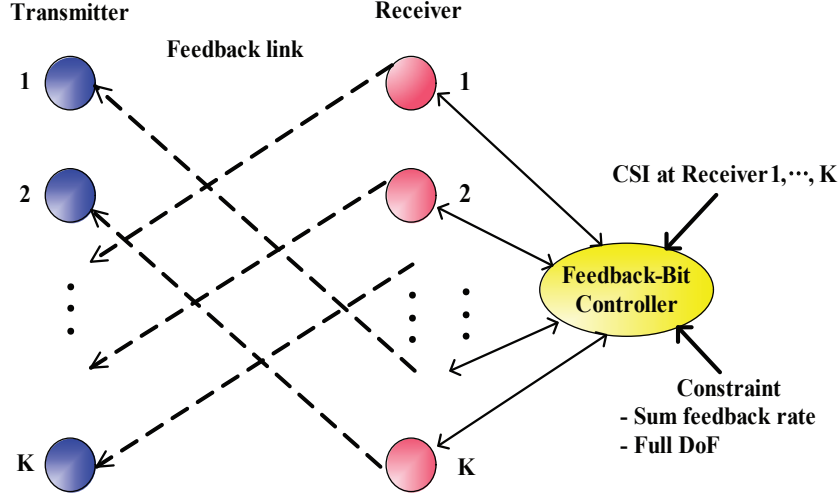


Fig. 6. Dynamic feedback-bits allocation scheme with the centralized bit controller

A. Dynamic Feedback-Bits Allocation for Minimizing Throughput Loss

The throughput loss is characterized by the sum of residual interference in (19). Therefore, we formulate the solution of dynamic feedback-bit allocation as following optimization problem :

$$\begin{aligned} \min_{\mathbf{B}} \quad & \sum_{k=1}^K E_{\mathcal{W}} \left(\hat{I}^{[k]} \right) \\ \text{s.t.} \quad & \sum_{k=1}^K B_k \leq B_T \end{aligned} \quad (26)$$

where $\mathbf{B} = \{B_1, \dots, B_K\}$ are the non-negative integers. Applying Proposition 1 and 2, (26) can be transformed to convex optimization problem :

$$\begin{aligned} \min_{\mathbf{B}} \quad & \sum_{k=1}^K a_k 2^{-\frac{B_k}{M-1}} \\ \text{s.t.} \quad & \sum_{k=1}^K B_k \leq B_T. \end{aligned} \quad (27)$$

Here, we define $\{a_k\}_{k=1}^K$ in modified CSI exchange topology as

$$\begin{cases} a_1 = \bar{\Gamma}(M) \cdot \left(Pd_{K1}^{-\alpha} \lambda_{max}^{[K1]} + Pd_{K-12}^{-\alpha} \lambda_{max}^{[K-11]} \right) \\ a_2 = \bar{\Gamma}(M) \cdot \left(Pd_{K-12}^{-\alpha} \lambda_{max}^{[K-12]} + Pd_{K1}^{-\alpha} \lambda_{max}^{[K2]} \right) \\ a_k = \bar{\Gamma}(M) \cdot Pd_{k-2k}^{-\alpha} \lambda_{max}^{[k-2k]} \quad k = 3, \dots, K \end{cases} \quad (28)$$

and $\{a_k\}_{k=1}^K$ in star feedback topology as

$$a_k = \bar{\Gamma}(M) \cdot \left(Pd_{\hat{k}k}^{-\alpha} \lambda_{max}^{[\hat{k}k]} + Pd_{\tilde{k}k}^{-\alpha} \lambda_{max}^{[\tilde{k}k]} \right) \quad k = 1, \dots, K \quad (29)$$

where $\hat{k} = \text{mod}(K + (k - 3), K) + 1$ and $\tilde{k} = \text{mod}(K + (k - 2), K) + 1$, respectively. In order to solve the constrained optimization problem in (27), we formulate the Lagrangian and take derivative with

respect to B_k . Then, we have

$$L = \sum_{k \in \mathcal{U}} a_k 2^{-\frac{B_k}{M-1}} + \nu \left(\sum_{k \in \mathcal{U}} B_k - B_T \right) \quad (30)$$

and

$$\frac{\partial L}{\partial B_k} = -2^{-\frac{B_k}{M-1}} \ln 2 \frac{a_k}{M-1} + \nu = 0, \quad (31)$$

where ν is the Lagrange multiplier and \mathcal{U} is the set of feedback links $\mathcal{U} = \{1, \dots, K\}$. From (31), we obtain B_k as

$$B_k = (M-1) \cdot \log_2 \left(\frac{\mu a_k}{M-1} \right) \quad (32)$$

under the following constraint

$$\sum_{k \in \mathcal{U}} (M-1) \cdot \log_2 \left(\frac{\mu a_k}{M-1} \right) = B_T, \quad (33)$$

where $\mu = \frac{\ln 2}{\nu}$. Combining (32) and (33) with $B_k \geq 0$, the number of optimal feedback-bit B_k^* that minimizes the sum residual interference is obtained as²

$$B_k^* = \frac{1}{|\mathcal{U}|} \left(\gamma - (M-1) \cdot |\mathcal{U}| \cdot \log_2 \left(\frac{M-1}{a_k} \right) \right)^+ \quad (34)$$

where $|\mathcal{U}|$ denotes the cardinality of \mathcal{U} and $\gamma = B_T + \sum_{k \in \mathcal{U}} (M-1) \cdot \log_2 \left(\frac{M-1}{a_k} \right)$. The solution of (34) is iteratively found through the waterfilling algorithm, which is described in Algorithm 3. However, the feedback-bits should become integer so that each of optimal feedback-bits $\{B_k^* : k \in \mathcal{U}\}$ is truncated to

$$B_k^* = \lfloor B_k^* \rfloor \quad (35)$$

where $\lfloor x \rfloor$ is the largest integer not greater than x .

- *Overhead of the dynamic feedback-bits allocation* : The computation of $\{B_k^* : k \in \mathcal{U}\}$ in (35) requires the set of interfering channel gains $\{a_k\}_{k=1}^K$ at the centralized bit controller, which consist of the variability of path-loss and small-scale fading. Since the gain of small-scale fading in $\{a_k\}_{k=1}^K$ shows the fast fluctuation, such a CSI should be collected to the bit controller over every transmission period. To reduce the burden of CSI exchange, assume that the network model where an individual node is distributed randomly and independently of each other. Then, the key factor of performance degradation becomes the randomly distributed cross-link distance $\{d_{kj}\}_{k \neq j}$ so that the bit controller may conduct feedback-bit allocation algorithm using the path loss which represents a slow variability

² $(a)^+$ implies that $(a)^+ = \begin{cases} a & \text{if } a \geq 0 \\ 0 & \text{if } a < 0 \end{cases}$.

Algorithm 3: Waterfilling Algorithm for Dynamic Feedback-Bit Allocation

```

 $i=0;$ 
 $U = \{1, \dots, K\};$ 
while  $i=0$  do
    Determine the water-level  $\gamma = B_T + \sum_{k \in U} (M-1) \cdot \log_2 \left( \frac{M-1}{a_k} \right).$ 
    Choose the user set  $k^* = \arg \max \left\{ \frac{M-1}{a_k} : k \in U \right\}.$ 
    if  $\gamma - (M-1) \cdot |U| \cdot \log_2 \left( \frac{M-1}{a_{k^*}} \right) \geq 0$  then  $\{B_k^* : k \in U\}$  is determined by (34).
     $i=i+1;$ 
    else Let define  $U = \{U \text{ except for } k^*\}$  and  $B_{k^*}^* = 0.$ 

```

compared with small-scale fading channel. The solution of feedback-bit allocation can be computed by Algorithm 3 by replacing $\{a_k\}_{k=1}^K$ with the following $\{\bar{a}_k\}_{k=1}^K$.

- 1) Modified CSI-exchange topology : Note that $\{\bar{a}_k\}_{k=1}^K$ is the expected value of $\{a_k\}_{k=1}^K$ in (28) over $\{\mathbf{H}^{[ij]}\}_{i,j=1}^K$. Then, \bar{a}_k is upper-bounded as ³

$$\bar{a}_k = \begin{cases} E_{\mathbf{H}}[a_1] \leq \bar{\Gamma}(M) \cdot (PM^2 d_{K1}^{-\alpha} + PM^2 d_{K-12}^{-\alpha}) \\ E_{\mathbf{H}}[a_2] \leq \bar{\Gamma}(M) \cdot (PM^2 d_{K-12}^{-\alpha} + PM^2 d_{K1}^{-\alpha}) \\ E_{\mathbf{H}}[a_k] \leq \bar{\Gamma}(M) \cdot PM^2 d_{k-2k}^{-\alpha} \quad k = 3, \dots, K. \end{cases} \quad (36)$$

- 2) Star feedback topology : From (29), we obtain $\{\bar{a}_k\}_{k=1}^K$ as below.

$$\bar{a}_k = E_{\mathbf{H}}[a_k] \leq \bar{\Gamma}(M) \cdot (PM^2 d_{kk}^{-\alpha} + PM^2 d_{kk}^{-\alpha}) \quad k = 1, \dots, K \quad (37)$$

From (36) and (37), the dynamic feedback-bits allocation is conducted by gathering a long-term CSI which requires the much longer feedback period rather than the cases of (28) and (29).

B. Scaling Law of Total Feedback Bits

Each pair of transmitter-receiver obtains the interference-free link for its desired data stream under the IA strategies. However, misaligned beamformers in limited feedback channel destroy the linear scaling gain of sum capacity, especially at high SNR regime. In this subsection, we analyze the total number of feedback-bits that achieve same DoF as the case of perfect CSI in proposed feedback topologies. To achieve linear scaling DoF in K -user interference channel, the sum of residual interference maintains the

³Note that $E_{\mathbf{H}}[\lambda_{\max}^{[ij]}] \leq M^2$, where $\lambda_{\max}^{[ij]}$ is a maximum eigenvalue of $\mathbf{H}^{[ij]}(\mathbf{H}^{[ij]})^H$.

constant value over whole SNR regimes according to

$$\begin{aligned}
DoF &= \lim_{P \rightarrow \infty} \frac{E_{\mathcal{W}}[R_{\text{limited}}]}{\log_2 P} \\
&= \lim_{P \rightarrow \infty} \frac{\sum_{k=1}^K E_{\mathcal{W}} \left[\log_2 \left(P d_{kk}^{-\alpha} |\hat{\mathbf{r}}^{[k]} \mathbf{H}^{[kk]} \hat{\mathbf{v}}^{[k]}|^2 \right) \right] - \sum_{i=1}^K E_{\mathcal{W}} [\log_2 (\hat{I}^{[k]})]}{\log_2 P} \\
&= \lim_{P \rightarrow \infty} \frac{\sum_{k=1}^K E_{\mathcal{W}} \left[\log_2 \left(P d_{kk}^{-\alpha} |\hat{\mathbf{r}}^{[k]} \mathbf{H}^{[kk]} \hat{\mathbf{v}}^{[k]}|^2 \right) \right]}{\log_2 P} - \lim_{P \rightarrow \infty} \frac{\sum_{k=1}^K E_{\mathcal{W}} [\log_2 (\hat{I}^{[k]})]}{\log_2 P} \\
&\leq K - \lim_{P \rightarrow \infty} \frac{\sum_{k=1}^K \log_2 (E_{\mathcal{W}} [\hat{I}^{[k]}])}{\log_2 P} \\
&\stackrel{(a)}{=} K
\end{aligned} \tag{38}$$

where (a) follows from the constant value of $\sum_{k=1}^K \log_2 (E_{\mathcal{W}} [\hat{I}^{[k]}])$.

Let denote B_T^* as the total feedback bits that achieve linearly scaling DoF with K . Then, we formulate the sum residual interference as an exponential function of a_k and B_k

$$\begin{aligned}
\sum_{k=1}^K \log_2 (E_{\mathcal{W}} [\hat{I}^{[k]}]) &\leq \sum_{k=1}^K \log_2 \left(a_k 2^{-\frac{B_k}{M-1}} \right) \\
&= \sum_{k=1}^K \log_2 (a_k) + \sum_{k=1}^K \log_2 \left(2^{-\frac{B_k}{M-1}} \right) \\
&= C
\end{aligned} \tag{39}$$

where $C > 0$ is constant. From (39), we obtain B_T^* as

$$\begin{aligned}
B_T^* &= \sum_{k=1}^K B_k \\
&= (M-1) \cdot \left(\sum_{k=1}^K \log_2 a_k - C \right) \\
&= K \cdot (M-1) \cdot \log_2 P + (M-1) \cdot \left(\sum_{k=1}^K \log_2 \hat{a}_k - C \right)
\end{aligned} \tag{40}$$

where $\hat{a}_k = \frac{a_k}{P}$, $\forall k$. Since the total feedback-bits is the non-negative integer, we determine B_T^* as

$$B_T^* = \text{nint}(B_T^*) \tag{41}$$

where $\text{nint}(x)$ is the nearest integer function of x .

- *Implementation of feedback-bits allocation* : In the centralized K -user interference channel such as star feedback topology, CSI-BS collects $\{a_k\}_{k=1}^K$ and computes B_T^* that achieves DoF of K . Given computed B_T^* , each of B_k^* is determined by Algorithm 3 and then $\mathbf{v}^{[k]}$ is quantized to $\hat{\mathbf{v}}^{[k]}$ by using B_k^* bits random vector codebook at CSI-BS. However, the proposed modified CSI-exchange scheme is conducted without any centralized controller. To implement the feedback-bits allocation in the distributed K -user networks, we modify the constraint in (39) into the individual constraints of k as below.

$$\log_2 (E_{\mathcal{W}} [\hat{I}^{[k]}]) \leq \log_2 \left(a_k 2^{-\frac{B_k}{M-1}} \right) = \frac{C}{K}, \quad \forall k. \tag{42}$$

Algorithm 4: Modified CSI exchange topology with the distributive feedback-bits allocation

-
- 1. Feedback of $\hat{\mathbf{v}}^{[1]}$ and $\hat{\mathbf{v}}^{[2]}$:** Assuming perfect CSI exchange between receiver $K - 1$ and K , k -th receiver computes $\mathbf{v}^{[k]}$ and the corresponding feedback bits B_k^{d*} , where $k = 1, 2$. Then, $\mathbf{v}^{[k]}$ is quantized to $\hat{\mathbf{v}}^{[k]}$ using B_k^{d*} bits codebook and fed back to the corresponding transmitter.
 - 2. Feedback of $\hat{\mathbf{v}}^{[3]}, \dots, \hat{\mathbf{v}}^{[K]}$**
- for $k=3:K$ do**
- $(k - 2)$ -th receiver calculates B_k^{d*} feedback bits and $\bar{\mathbf{v}}^{[k]}$. Then, $\bar{\mathbf{v}}^{[k]}$ is quantized to $\hat{\mathbf{v}}^{[k]}$ and fed
 - back to the transmitter k .
-

Then, the required feedback bits B_k^{d*} for k -th beamformer that achieve a linear scaling law are derived as

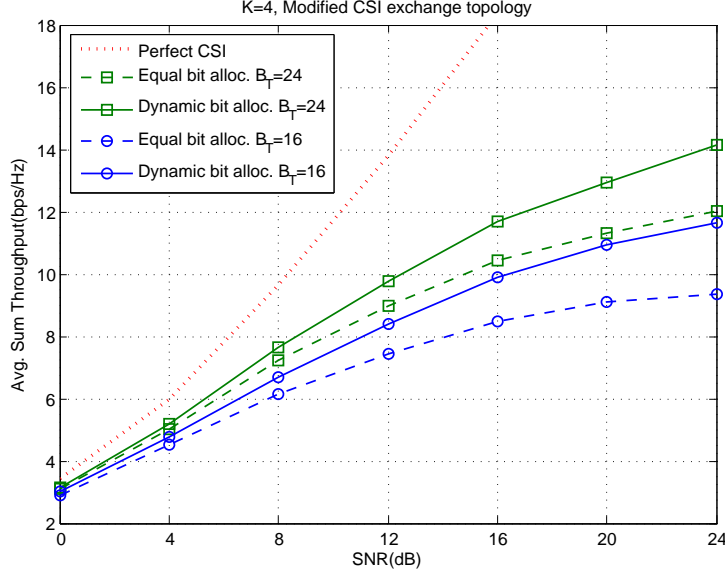
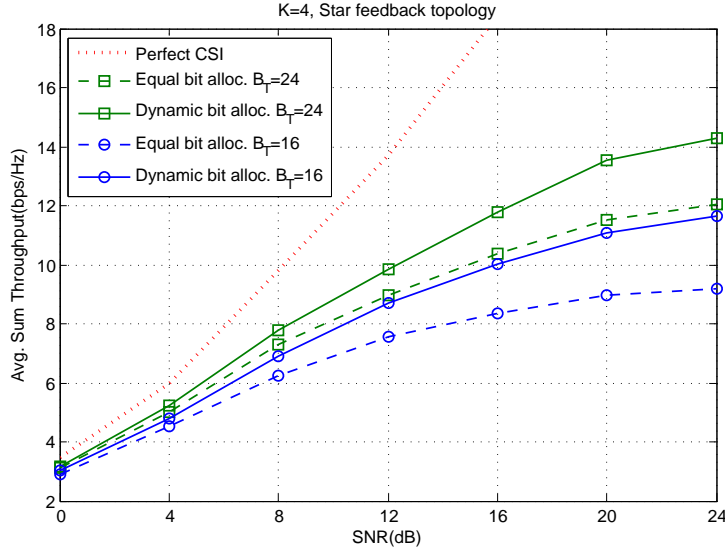
$$B_k^{d*} = \text{nint}(B_k^d) \quad (43)$$

where $B_k^d = (M - 1) \cdot (\log_2 a_k - \frac{C}{K})$. From the components that consists of a_k in (28), B_{K-1}^{d*} and B_K^{d*} are computed under the assumption of CSI exchange between receiver $K - 1$ and K and other B_k^{d*} is computed with local channel knowledge at receiver k . Based on (43), we design the modified CSI exchange scheme with the distributive feedback-bits allocation, which achieves linearly scaling DoF with K in limited feedback channel. The procedure is represented in Algorithm 4.

VI. NUMERICAL RESULTS

In this section, we represent the performance of proposed IA feedback topologies in K -user MIMO interference channel with limited feedback. The throughput improvement of dynamic feedback-bits allocation in the different feedback topologies is verified comparing with the conventional case of *equal feedback-bit allocation* for which the number of feedback-bits sent to each transmitter is equal and fixed. Also, the scaling law of total feedback-bits that achieves same DoF as the case of perfect CSI is shown in both centralized and distributed K -user network models.

Fig. 7 and Fig. 8 show the average sum throughput of 4-user 3×3 MIMO IA channel in limited feedback channel, which are constructed by modified CSI-exchange and star feedback topology with the dynamic feedback-bits algorithm proposed in section V.A. For comparison, the curve for equal feedback-bit allocation is also plotted. We set the parameters $B_T = 16$ and 24 , $\alpha = 3.8$ and the ratio between the distance of interference link and desired link, $(d_{kj}/d_{kk})_{k \neq j} = 1$. While the dynamic feedback-bits allocation scheme requires the centralized feedback-bits controller, it shows superior performance of sum throughput than equal feedback-bits allocation scheme. The performance gap between dynamic and equal


 Fig. 7. Average sum throughput of modified CSI-exchange topology in $B_T=16$ and 24.

 Fig. 8. Average sum throughput of star feedback topology in $B_T=16$ and 24.

bit allocation becomes larger in high SNR since the proposed feedback-bits allocation effectively regulates the strong residual interference. In Fig. 9, the performance gains of dynamic feedback-bit allocation in $B_T = 16$ and 24 are compared in the modified CSI-exchange topology. The measure of the gain of feedback-bits allocation is denoted as the difference between sum throughput in dynamic and equal bit allocation:

$$G = \frac{R_{\text{limited}}^{\text{dynamic}} - R_{\text{limited}}^{\text{equal}}}{R_{\text{limited}}^{\text{equal}}} \times 100. \quad (44)$$

We figure out that the gain of feedback-bits allocation in $B_T = 16$ is larger than $B_T = 24$ constraint so

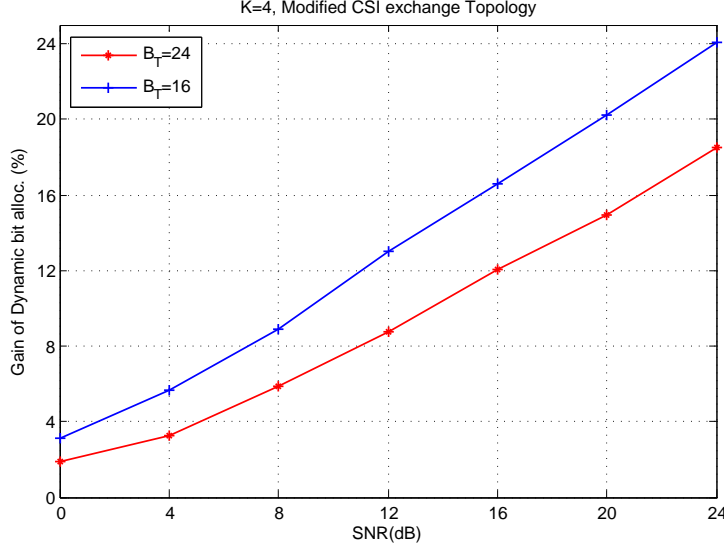


Fig. 9. Ratio of the performance enhancement of dynamic bit allocation in modified CSI-exchange topology.

that the dynamic feedback-bits allocation strategy is more effective in lower rate feedback environments. In other words, the performance gain of waterfilling solution becomes dominant within the range of low water-levels γ .

In Fig. 10, we compare the average sum throughput of dynamic feedback-bits allocation based on the long-term CSI of $\{\bar{a}_k\}_{k=1}^K$ with that of equal feedback-bits allocation given $B_T = 16$ and 20. Assuming each pair of transmitter-receiver is uniformly distributed within the range of $(d_{kj}/d_{kk})_{k \neq j} \in [0.5 \ 1.5]$, the dynamic feedback-bits allocation scheme acquires the better throughput compared with equal feedback-bits allocation scheme. Since the dynamic feedback-bits allocation determines the number of quantization bits by using path-loss, it does not requires the frequent exchange of CSI between receivers and the feedback-bits controller. This provides the benefit of lower cost for implementation.

In Fig. 7, 8 and 10, we find that a linearly scaling DoF can not be achieved in high SNR regimes since the given B_T feedback-bits are not enough to manage the strong residual interference. In (40) and (43), we suggest that the required total feedback bits that achieve linear scaling law of sum throughput in both centralized and distributed manners. Fig.11 shows the performance of sum throughput under the following two feedback-bits allocation scheme based on (40) and (43):

- 1) Centralized bit allocation strategy : It assumes that the centralized controller collects all cross-link gains $\{a_k\}_{k=1}^K$ and computes B_T^* using (40). Each of B_k^* is computed by the dynamic feedback-bits allocation scheme in Algorithm 3.
- 2) Distributed bit allocation strategy: Each B_k^{d*} is sequentially computed based on the local CSI at receiver k . Details are described in Algorithm 4.

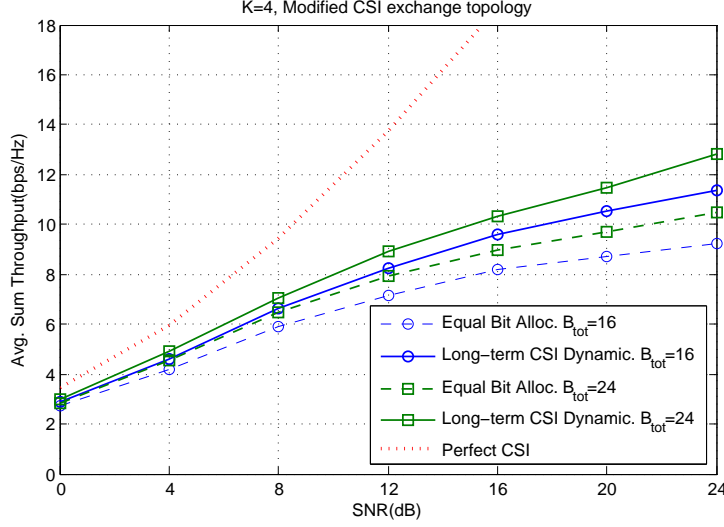


Fig. 10. Average sum throughput of modified CSI-exchange topology in randomly distributed user locations

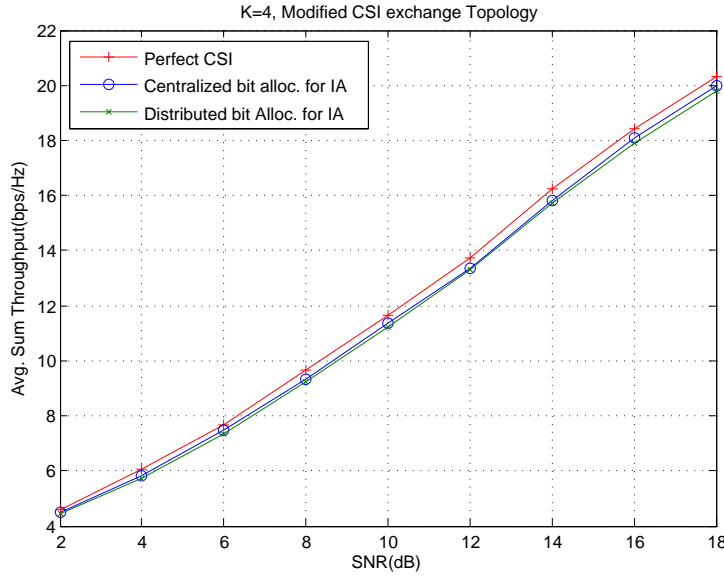


Fig. 11. Scaling law of sum throughput in limited feedback channel

Setting the parameters $C_{dB} = 3dB$ and $(d_{kj}/d_{kk})_{k \neq j} = 2$, the sum throughput in both two schemes shows linear increase over the whole SNR region while 1) slightly provides better performance than 2). Also, the total feedback-bits in both 1) and 2) are linearly increased with K and logarithmically increased with P .

VII. CONCLUSION

In this paper, the efficient feedback topologies for IA have been proposed in K -user MIMO interference channels. We showed that the proposed feedback topologies provide the dramatic reduction of network

overhead compared with a conventional feedback framework for IA. In the context of limited feedback channel, we analyzed the upper bounds of sum residual interference in given feedback topologies which are equivalent to the sum throughput loss due to the quantization error. Using these bounds, we suggested the dynamic feedback-bits allocation scheme that minimizes sum residual interference with the water filling solution. The performance gain of dynamic feedback-bits allocation was dominant in high SNR regions while each of receiver is affected by a strong residual interference. Furthermore, the scaling law of feedback bits achieving IA is derived, which is linearly increased with $K(M - 1)$ and $\log_2 P$. For the practical implementation, we developed the feedback-bits allocation scheme that only requires the long-term channel gains and distributive feedback-bits controlling system without any centralized controller.

APPENDIX A

PROOF OF LEMMA 1

From (13), the expected squared norm of $\Delta \mathbf{v}^{[k]}$ is bounded as

$$\begin{aligned}
 E \left[\left\| \Delta \mathbf{v}^{[k]} \right\|^2 \right] &= E \left[\left\| \mathbf{v}^{[k]} - \hat{\mathbf{v}}^{[k]} \right\|^2 \right] \\
 &= 2E \left[\left\| \mathbf{v}^{[k]} \right\|^2 \right] - 2E \left[\text{Re} \langle \mathbf{v}^{[k]}, \hat{\mathbf{v}}^{[k]} \rangle \right] \\
 &\leq 2E \left[\left\| \mathbf{v}^{[k]} \right\|^2 \right] - 2E \left[\left| \mathbf{v}^{[k] \dagger} \hat{\mathbf{v}}^{[k]} \right| \right] \\
 &= 2 - 2E[\cos \theta] \\
 &= 2E[1 - \cos \theta] \\
 &\leq 2E[1 - \cos^2 \theta] \\
 &= 2E[\sin^2 \theta]
 \end{aligned} \tag{45}$$

where $\text{Re} \langle, \rangle$ denotes a real value of inner product between two vectors.

Using the result from Dai *et al.*[30],

$$E[\sin^2 \theta] \leq \frac{2\Gamma\left(\frac{1}{M-1}\right)}{M-1} \cdot 2^{-\frac{B}{M-1}}. \tag{46}$$

Applying (46) into (45), we obtain the desired result.

APPENDIX B

PROOF OF PROPOSITION 1

Consider the residual interference at receiver $K - 1$ and K affected by a misalignment between the interference from transmitter 1 and 2. From the design of $\hat{\mathbf{r}}^{[K-1]}$ on the $K - 2$ dimensional nullspace of

$\{\mathbf{H}^{[K-1k]}\hat{\mathbf{v}}^{[k]} | 1 \leq k \leq K, k \neq 2, K-1\}$, the $\hat{I}^{[K-1]}$ is derived as

$$\begin{aligned}
\hat{I}^{[K-1]} &= P \left| \sum_{k=1, k \neq K-1}^K d_{K-1k}^{-\alpha/2} \hat{\mathbf{r}}^{[K-1]\dagger} \mathbf{H}^{[K-1k]} \hat{\mathbf{v}}^{[k]} \right|^2 \\
&= P d_{K-12}^{-\alpha} \left| \hat{\mathbf{r}}^{[K-1]\dagger} \mathbf{H}^{[K-12]} \hat{\mathbf{v}}^{[2]} \right|^2 \\
&= P d_{K-12}^{-\alpha} \left| \hat{\mathbf{r}}^{[K-1]\dagger} \mathbf{H}^{[K-12]} \mathbf{v}^{[2]} - \sigma_2 \hat{\mathbf{r}}^{[K-1]\dagger} \mathbf{H}^{[K-12]} \Delta \bar{\mathbf{v}}^{[2]} \right|^2 \\
&\stackrel{(a)}{=} P d_{K-12}^{-\alpha} \left| \hat{\mathbf{r}}^{[K-1]\dagger} \mathbf{H}^{[K-11]} \mathbf{v}^{[1]} - \sigma_2 \hat{\mathbf{r}}^{[K-1]\dagger} \mathbf{H}^{[K-12]} \Delta \bar{\mathbf{v}}^{[2]} \right|^2 \\
&\stackrel{(b)}{\leq} P d_{K-12}^{-\alpha} \sigma_1^2 \left| \hat{\mathbf{r}}^{[K-1]\dagger} \mathbf{H}^{[K-11]} \Delta \bar{\mathbf{v}}^{[1]} \right|^2 + P d_{K-12}^{-\alpha} \sigma_2^2 \left| \hat{\mathbf{r}}^{[K-1]\dagger} \mathbf{H}^{[K-12]} \Delta \bar{\mathbf{v}}^{[2]} \right|^2 \\
&\stackrel{(c)}{\leq} P d_{K-12}^{-\alpha} \sigma_1^2 \left\| \hat{\mathbf{r}}^{[K-1]\dagger} \mathbf{H}^{[K-11]} \right\|^2 \left\| \Delta \bar{\mathbf{v}}^{[1]} \right\|^2 + P d_{K-12}^{-\alpha} \sigma_2^2 \left\| \hat{\mathbf{r}}^{[K-1]\dagger} \mathbf{H}^{[K-12]} \right\|^2 \left\| \Delta \bar{\mathbf{v}}^{[2]} \right\|^2
\end{aligned} \tag{47}$$

where (a) and (b) follow from $\text{span}(\mathbf{H}^{[K-11]} \mathbf{v}^{[1]}) = \text{span}(\mathbf{H}^{[K-12]} \mathbf{v}^{[2]})$ and $\hat{\mathbf{r}}^{[K-1]\dagger} \mathbf{H}^{[K-11]} \hat{\mathbf{v}}^{[1]} = 0$, respectively. Also, (c) is upper-bounded by Cauchy-Schwarz inequality⁴. Then, the expectation of $\hat{I}^{[K-1]}$ over \mathcal{W} is upper-bounded by

$$E_{\mathcal{W}} \left(\hat{I}^{[K-1]} \right) \leq P d_{K-12}^{-\alpha} \sigma_1^2 \lambda_{\max}^{[K-11]} + P d_{K-12}^{-\alpha} \sigma_2^2 \lambda_{\max}^{[K-12]}, \tag{48}$$

where $\left\| \hat{\mathbf{r}}^{[K-1]\dagger} \mathbf{H}^{[K-1k]} \right\|^2 \leq \lambda_{\max}^{[K-1k]}$, $k = 1, 2$.

Similarly, $\hat{\mathbf{r}}^{[K]}$ is designed on the nullspace of $\{\mathbf{H}^{[K-1k]}\hat{\mathbf{v}}^{[k]} | 1 \leq k \leq K, k \neq 1, K\}$ and then $\hat{I}^{[K]}$ is derived as

$$\begin{aligned}
\hat{I}^{[K]} &= P \left| \sum_{k=1, k \neq K}^K d_{Kk}^{-\alpha/2} \hat{\mathbf{r}}^{[K]\dagger} \mathbf{H}^{[Kk]} \hat{\mathbf{v}}^{[k]} \right|^2 \\
&= P d_{K1}^{-\alpha} \left| \hat{\mathbf{r}}^{[K]\dagger} \mathbf{H}^{[K1]} \hat{\mathbf{v}}^{[1]} \right|^2 \\
&= P d_{K1}^{-\alpha} \left| \hat{\mathbf{r}}^{[K]\dagger} \mathbf{H}^{[K1]} \mathbf{v}^{[1]} - \sigma_1 \hat{\mathbf{r}}^{[K]\dagger} \mathbf{H}^{[K1]} \Delta \bar{\mathbf{v}}^{[1]} \right|^2 \\
&= P d_{K1}^{-\alpha} \left| \hat{\mathbf{r}}^{[K]\dagger} \mathbf{H}^{[K2]} \mathbf{v}^{[2]} - \sigma_1 \hat{\mathbf{r}}^{[K]\dagger} \mathbf{H}^{[K1]} \Delta \bar{\mathbf{v}}^{[1]} \right|^2 \\
&\leq P d_{K1}^{-\alpha} \sigma_2^2 \left| \hat{\mathbf{r}}^{[K]\dagger} \mathbf{H}^{[K2]} \Delta \bar{\mathbf{v}}^{[2]} \right|^2 + P d_{K1}^{-\alpha} \sigma_1^2 \left| \hat{\mathbf{r}}^{[K]\dagger} \mathbf{H}^{[K1]} \Delta \bar{\mathbf{v}}^{[1]} \right|^2 \\
&\leq P d_{K1}^{-\alpha} \sigma_2^2 \left\| \hat{\mathbf{r}}^{[K]\dagger} \mathbf{H}^{[K2]} \right\|^2 \left\| \Delta \bar{\mathbf{v}}^{[2]} \right\|^2 + P d_{K1}^{-\alpha} \sigma_1^2 \left\| \hat{\mathbf{r}}^{[K]\dagger} \mathbf{H}^{[K1]} \right\|^2 \left\| \Delta \bar{\mathbf{v}}^{[1]} \right\|^2.
\end{aligned} \tag{49}$$

Then, the expectation of $\hat{I}^{[K]}$ over \mathcal{W} is represented as

$$E_{\mathcal{W}} \left(\hat{I}^{[K]} \right) \leq P d_{K1}^{-\alpha} \sigma_2^2 \lambda_{\max}^{[K2]} + P d_{K1}^{-\alpha} \sigma_1^2 \lambda_{\max}^{[K1]}. \tag{50}$$

From the CSI-exchange topology, following $\bar{\mathbf{v}}^{[k+2]}$ is designed on the subspace of $\mathbf{H}^{[kk+2]-1} \mathbf{H}^{[kk+1]} \hat{\mathbf{v}}^{[k+1]}$ and fed back to transmitter $k+2$ through B_{k+2} bits feedback channel at receiver k , where $k = 1, \dots, K-2$. Therefore, the quantized $\hat{\mathbf{v}}^{[k+2]}$ causes the misalignment between interference from transmitter $k+1$ and

⁴Note that $|\mathbf{a}^\dagger \mathbf{b}|^2 \leq \|\mathbf{a}\|^2 \|\mathbf{b}\|^2$, where $\mathbf{a}, \mathbf{b} \in \mathcal{C}^{M \times 1}$

$k + 2$ which generates the residual interference at receiver k . Then, we derive $\hat{I}^{[k]}$ as

$$\begin{aligned}
\hat{I}^{[k]} &= P \left| \sum_{m=1, m \neq k}^K d_{km}^{-\alpha/2} \hat{\mathbf{r}}^{[k]\dagger} \mathbf{H}^{[km]} \hat{\mathbf{v}}^{[m]} \right|^2 \\
&= P d_{kk+2}^{-\alpha} \left| \hat{\mathbf{r}}^{[k]\dagger} \mathbf{H}^{[kk+2]} \hat{\mathbf{v}}^{[k+2]} \right|^2 \\
&= P d_{kk+2}^{-\alpha} \left| \hat{\mathbf{r}}^{[k]\dagger} \mathbf{H}^{[kk+2]} \hat{\mathbf{v}}^{[k+2]} - \sigma_{k+2} \hat{\mathbf{r}}^{[k]\dagger} \mathbf{H}^{[kk+2]} \Delta \mathbf{v}^{[k+2]} \right|^2 \\
&= P d_{kk+2}^{-\alpha} \sigma_{k+2}^2 \left| \hat{\mathbf{r}}^{[k]\dagger} \mathbf{H}^{[kk+2]} \Delta \mathbf{v}^{[k+2]} \right|^2 \\
&\leq P d_{kk+2}^{-\alpha} \sigma_{k+2}^2 \left\| \hat{\mathbf{r}}^{[k]\dagger} \mathbf{H}^{[kk+2]} \right\|^2 \left\| \Delta \mathbf{v}^{[k+2]} \right\|^2
\end{aligned} \tag{51}$$

where $\hat{\mathbf{r}}^{[k]}$ is on the nullspace of $\{\mathbf{H}^{[km]} \hat{\mathbf{v}}^{[m]} | 1 \leq m \leq K, m \neq k, k+2\}$. From this result, the expectation of $\hat{I}^{[k]}$ is upper-bounded by

$$E_{\mathcal{W}} \left(\hat{I}^{[k]} \right) \leq P d_{kk+2}^{-\alpha} \sigma_{k+2}^2 \lambda_{\max}^{[kk+2]}. \tag{52}$$

APPENDIX C

PROOF OF PROPOSITION 2

In a star feedback topology, the design of IA precoders follows from (4). From the IA condition in (3), the interference from transmitter $k+1$ and $k+2$ is aligned on the same subspace at receiver k , where $k = 1, \dots, K-2$. However, a finite-rate feedback channel from CSI-BS to the corresponding transmitters cause the quantization error of beamformers so that the residual interference is generated by both quantized $\hat{\mathbf{v}}^{[k+1]}$ and $\hat{\mathbf{v}}^{[k+2]}$ at receiver k . Then, we derive $\hat{I}^{[k]}$ as

$$\begin{aligned}
\hat{I}^{[k]} &= P \left| \sum_{m=1, m \neq k}^K d_{km}^{-\alpha/2} \hat{\mathbf{r}}^{[k]\dagger} \mathbf{H}^{[km]} \hat{\mathbf{v}}^{[m]} \right|^2 \\
&= P d_{kk+2}^{-\alpha} \left| \hat{\mathbf{r}}^{[k]\dagger} \mathbf{H}^{[kk+2]} \hat{\mathbf{v}}^{[k+2]} \right|^2 \\
&= P d_{kk+2}^{-\alpha} \left| \hat{\mathbf{r}}^{[k]\dagger} \mathbf{H}^{[kk+2]} \mathbf{v}^{[k+2]} - \sigma_{k+2} \hat{\mathbf{r}}^{[k]\dagger} \mathbf{H}^{[kk+2]} \Delta \mathbf{v}^{[k+2]} \right|^2 \\
&= P d_{kk+2}^{-\alpha} \left| \hat{\mathbf{r}}^{[k]\dagger} \mathbf{H}^{[kk+1]} \mathbf{v}^{[k+1]} - \sigma_{k+2} \hat{\mathbf{r}}^{[k]\dagger} \mathbf{H}^{[kk+2]} \Delta \mathbf{v}^{[k+2]} \right|^2 \\
&\leq P d_{kk+2}^{-\alpha} \sigma_{k+1}^2 \left\| \hat{\mathbf{r}}^{[k]\dagger} \mathbf{H}^{[kk+1]} \right\|^2 \left\| \Delta \mathbf{v}^{[k+1]} \right\|^2 + P d_{kk+2}^{-\alpha} \sigma_{k+2}^2 \left\| \hat{\mathbf{r}}^{[k]\dagger} \mathbf{H}^{[kk+2]} \right\|^2 \left\| \Delta \mathbf{v}^{[k+2]} \right\|^2
\end{aligned} \tag{53}$$

where $\hat{\mathbf{r}}^{[k]}$ is designed on the nullspace of $\{\mathbf{H}^{[km]} \hat{\mathbf{v}}^{[m]} | 1 \leq m \leq K, m \neq k, k+2\}$. From this result, the expectation of $\hat{I}^{[k]}$ is upper-bounded by

$$E_{\mathcal{W}} \left(\hat{I}^{[k]} \right) \leq P d_{kk+2}^{-\alpha} \sigma_{k+1}^2 \lambda_{\max}^{[kk+1]} + P d_{kk+2}^{-\alpha} \sigma_{k+2}^2 \lambda_{\max}^{[kk+2]}. \tag{54}$$

In the same manner, a pair of interference from transmitter 1 and K and transmitter 1 and 2 incur the residual interference at receiver $K-1$ and K , respectively. Applying above analysis, we represent the expected residual interference at receiver $K-1$ and K as follows.

$$\begin{aligned}
E_{\mathcal{W}} \left(\hat{I}^{[K-1]} \right) &\leq P d_{K-11}^{-\alpha} \sigma_K^2 \lambda_{\max}^{[K-1K]} + P d_{K-11}^{-\alpha} \sigma_1^2 \lambda_{\max}^{[K-11]} \\
E_{\mathcal{W}} \left(\hat{I}^{[K]} \right) &\leq P d_{K2}^{-\alpha} \sigma_1^2 \lambda_{\max}^{[K1]} + P d_{K2}^{-\alpha} \sigma_2^2 \lambda_{\max}^{[K2]}.
\end{aligned} \tag{55}$$

REFERENCES

- [1] V. R. Cadambe and S. A. Jafar, "Interference alignment and the degrees of freedom for the K user interference channel," *IEEE Trans. on Inform. Theory*, vol. 54, no. 8, pp. 3425-3441, Aug. 2008.
- [2] M. Shen, A. Hst-Madsen, and J. Vidal, "An improved interference alignment scheme for frequency selective channels," in *Proc., IEEE Int. Symp. Inform. Theory*, Jul. 2008.
- [3] S. W. Choi, S. A. Jafar, and S. Y. Chung, "On the beamforming design for efficient interference alignment," *IEEE Commun. Lett.*, vol. 13, no. 11, pp. 847-849, Nov. 2009.
- [4] T. Gou and S. A. Jafar, "Degrees of freedom of the K user MxN MIMO interference channel," *IEEE Trans. on Inform. Theory*, vol. 56, no. 12, pp. 6040-6057, Dec. 2010.
- [5] A. Ghasemi, A. S. Motahari, and A. K. Khandani, "Interference alignment for the K User MIMO Interference Channel," in *Proc., IEEE Int. Symp. Inform. Theory*, June. 2010.
- [6] C. M. Yetis, T. Gou, S. A. Jafar and A. H. Kayran, "Feasibility conditions for Interference Alignment," in *Proc., IEEE GLOBECOM*, Nov. 2009.
- [7] F. Negro*, S. P. Shenoy, D. T. M. Slock and I. Ghauri, "Interference alignment limits for K-user frequency-flat MIMO interference channels," *17th European Signal Process. Conf.*, Aug. 2009.
- [8] G. Bresler, D. Cartwright and D. Tse, "Settling the feasibility of interference alignment for the MIMO interference channel: the symmetric square case," available at <http://arxiv.org/abs/1104.0888>, Apr. 2011.
- [9] S. W. Peters and R. W. Heath, Jr., "Interference alignment via alternating minimization," in *Proc., IEEE Int. Conf. on Acoustics, Speech and Signal Process.*, Apr. 2009.
- [10] K. Gomadam, V. Cadambe, and S. Jafar, "Approaching the capacity of wireless networks through distributed interference alignment," in *Proc., IEEE GLOBECOM*, Dec. 2008.
- [11] C. Suh and D. Tse, "Interference alignment for cellular networks," in *Proc., Allerton Conf. on Comm., Cont., and Comp.*, 2009.
- [12] C. Suh, M. Ho, and D. Tse, "Downlink Interference Alignment," submitted to *IEEE Trans. on Commun.*, May. 2010. (Available: <http://arxiv.org/abs/1003.3707>)
- [13] N. Lee, W. Shin, and B. Clerckx, "Interference Alignment with Limited Feedback on Two-cell Interfering Two-User MIMO-MAC," submitted to *Proc., IEEE Int. Conf. on Commun.*, June. 2011. (Available: <http://arXiv.org/abs/1003.0933>)
- [14] R. Tresch and M. Guillaud, "Cellular interference alignment with imperfect channel knowledge," in *Proc., IEEE Int. Conf. on Commun.*, June. 2009.
- [15] J. Thukral and H. Bolcskei, "Interference alignment with limited feedback," in *Proc., IEEE Int. Symp. Inform. Theory*, June. 2009.
- [16] R. T. Krishnamachari and M. K. Varanasi, "Interference alignment under limited feedback for MIMO interference channels," submitted to *IEEE Trans. on Inform. Theory*, Nov. 2009. (Available: <http://arxiv.org/abs/0911.5509>)
- [17] D. J. Love, R. W. Heath, Jr. and T. Strohmer, "Grassmannian beamforming for multiple-input multiple-output wireless systems," *IEEE Trans. on Inform. Theory*, vol. 49, no. 10, pp. 2735-2747, Oct. 2003.
- [18] K. K. Mukkavilli, A. Sabharwal, E. Erkip and B. Aazhang, "On beamforming with finite rate feedback in multiple antenna systems," *IEEE Trans. on Inform. Theory*, vol. 49, no. 10, pp. 2562-2579, Oct. 2003.
- [19] D. J. Love and R. W. Heath, Jr., "Limited feedback unitary precoding for orthogonal space-time block codes," *IEEE Trans. on Signal Process.*, vol. 53, no. 1, pp. 64-73, Jan. 2005.
- [20] D. J. Love and R. W. Heath, Jr., "Limited feedback unitary precoding for spatial multiplexing systems," *IEEE Trans. on Inform. Theory*, vol. 51, no.8, pp. 1967-1976, Aug. 2005.

- [21] C. K. Au-Yeung and D. J. Love, "On the Performance of Random Vector Quantization Limited Feedback Beamforming in a MISO System," *IEEE Trans. on Wireless Commun.*, vol. 6, no. 2, pp. 458-462, Feb. 2007.
- [22] N. Jindal, "MIMO broadcast channels with finite-rate feedback," *IEEE Trans. on Inform. Theory*, vol. 52, no. 11, pp. 5045–5060, Nov. 2006.
- [23] T. Yoo, N. Jindal and A. Goldsmith, "Multi-antenna downlink channels with Limited feedback and user selection," *IEEE Journal on Sel. Areas in Commun.*, vol. 25, no. 7, pp. 1478-1491, Sep. 2007.
- [24] N. Ravindran and N. Jindal, "Limited feedback-based block diagonalization for the MIMO broadcast channel," *IEEE Journal on Sel. Areas in Commun.*, vol. 26, no. 8, pp. 1473-1482, Oct. 2008.
- [25] W. Shin, N. Lee, J. Lim, C. Shin and K. Jang, "Interference Alignment Through User Cooperation for Two-cell MIMO Interfering Broadcast Channels," in *Proc., IEEE GLOBECOM*, Dec. 2010.
- [26] *IEEE C802.16-10/0009, Future wireless broadband networks: challenges and possibilities*, Jan. 2010.
- [27] R. Tresch, M. Guillaud, and E. Riegler, "On the achievability of interference alignment in the K-User constant MIMO interference channel," in *Proc., IEEE Workshop on Statistical Signal Process.*, Sep. 2009.
- [28] J. Zhang and J. G. Andrews, "Adaptive spatial intercell interference cancellation in multicell wireless networks," *IEEE Journal on Sel. Areas in Commun.*, vol. 28, no. 9, pp. 1455-1468, Dec. 2010.
- [29] R. Bhagavatula and R. W. Heath, Jr, "Adaptive limited feedback for sum-rate maximizing beamforming in cooperative multicell systems," *IEEE Trans. on Signal Process.*, vol. 59, no. 2, pp. 800-811, Feb. 2011.
- [30] W. Dai, Y.Liu, and B. Rider, "Quantization bounds on Grassmann manifolds of arbitrary dimensions and MIMO communications with feedback," in *Proc., IEEE GLOBECOM*, Nov. 2005.
- [31] A. Nusairat, X. Y. Li and S. K. Makki, "Qos-Aware Integrated Cellular and WiFi Wireless Networks," *IEEE/NSF WTASA*, Jun. 2007.